# A high resolution, high frame rate detector based on a microchannel plate read out with the Medipix2 counting CMOS pixel chip

Bettina Mikulec, *Member, IEEE,* John V. Vallerga, Jason B. McPhate, Anton S. Tremsin, *Member, IEEE,* Oswald H. W. Siegmund, Allan G. Clark

*(Invited Paper)*



***Abstract*— The future of ground-based optical astronomy lies with advancements in adaptive optics (AO) to overcome the limitations that the atmosphere places on high resolution imaging. A key technology for AO systems on future very large telescopes are the wavefront sensors (WFS) which detect the optical phase error and send corrections to deformable mirrors. Telescopes with >30 m diameters will require WFS detectors that have large pixel formats (512×512), low noise (<3 $e^-$/pixel) and very high frame rates (∼1 kHz). These requirements have led to the idea of a bare CMOS active pixel device (the Medipix2 chip) functioning in counting mode as an anode with noiseless readout for a microchannel plate (MCP) detector and at 1 kHz continuous frame rate. First measurement results obtained with this novel detector are presented both for UV photons and beta particles.**

***Index Terms*— adaptive optics, wavefront sensor, photon counting, CMOS pixel chip, microchannel plate detector, high frame rate.**

## I. Introduction

GROUND-BASED astronomy in the optical and infrared spectral regions suffers from distortions of the incoming wave-fronts by the atmosphere. Turbulence combined with pressure and more importantly with temperature gradients yield slightly different refractive indices of the patches of air that the wave-fronts traverse. Consequently, the resulting phase errors give rise to a blurred image at the telescope focal plane. Ideally, the angular resolution of a telescope would only be limited by the diffraction limit of the primary mirror that is proportional to $\lambda/D$. But even at good observing sites the coherence length in the atmospheric layers is only around 20 cm; thus it would not help to use primary mirrors with a diameter $D$ larger than that (except for the increased light collection).

It is therefore essential for large telescopes to use a system that compensates for atmospheric distortions. Such a system is called an adaptive optics (AO) system. It adjusts the phase of the incoming wave-front using deformable mirrors to provide compensation for the phase distortion. The three main parts of an AO system are shown in Fig. 1: the deformable mirror, the wavefront sensor (WFS) and the control electronics. The system needs a bright reference star whose light traverses approximately the same path through the atmosphere as the light from the object to be studied. Since bright reference stars are not usually situated close to the object being studied, powerful lasers projected into the sky are used as artificial guide stars. Laser guide stars rely on the light from a laser being backscattered to the telescope, and thus sampling the atmosphere below the scattering location. Rayleigh guide stars use Rayleigh scattering in the atmosphere, while Sodium guide stars use the resonant scattering of sodium atoms present in a thin layer at ∼90 km height [1]. The distorted wave-front from distant objects and these beacons are collected by the telescope, and the collimated beam is reflected by a deformable mirror. The beamsplitter (most current ground-based AO astronomy uses optical light for wavefront sensing while passing the infrared to the science camera) divides up the light into the scientific path with a high-resolution camera at its end and into the wavefront sensing path. There the WFS measures the phase distribution in the optical beam. Its signals are subsequently used to calculate in a control computer the necessary compensation, which is applied to the deformable mirror via so-called actuators. This closes the loop and another correction cycle starts. The frequency of this cycle (on the order of 100 to 1000 Hz) should be much higher than the atmospheric changes [1].

Various methods exist to measure the phase error with the WFS. A Shack-Hartmann WFS, for example, samples the pupil plane of the beacon by an array of sub-apertures. In the case of a non-distorted incoming wavefront this would yield an image of regularly spaced light spots in the image plane (Fig. 2). Distortions in the incoming wavefront lead to a movement of the spots. Thus the centroid position carries information about the first derivative of the wavefront phase and is used to determine the correction sent to the deformable mirror.

### A. Wavefront sensor requirements for future large telescopes

Most modern ground-based telescopes like the big 5-10 m telescopes on Mauna Kea, Hawaii, or the European Southern Observatory (ESO) telescopes in Chile are already equipped

B. Mikulec and A. Clark are with the University of Geneva, Switzerland (e-mail: bettina.mikulec@cern.ch).

J. Vallerga, J. McPhate, A. Tremsin and O. Siegmund are with the Space Science Laboratory, University of California, Berkeley, California.

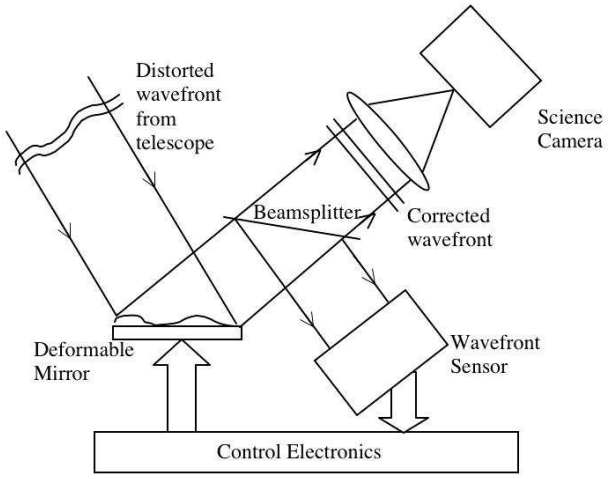


Fig. 1. Schematic diagram of an AO system. The distorted wavefront is corrected by a deformable mirror. A beamsplitter sends the light from a bright guide star to the WFS that measures the distortion. From this information the control computer calculates the new values for the correction and sends signals to the actuators that modify the deformable mirror such that it cancels the distortions.

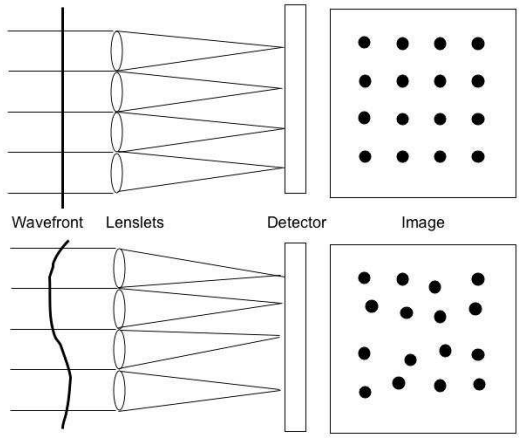


Fig. 2. Shack-Hartmann wavefront sensing method: An input plane wave (top) is focused by a lenslet array onto a 2D detector yielding a regularly spaced array of spots. If the wavefront is distorted (bottom), the spots move away from the 'ideal' position. This movement of the centroids is a measure of the wavefront slope.

with AO systems. Currently, the next generation of large telescopes is under intense study. Telescopes are planned with primary mirror diameters ranging from 30 m up to 100 m (the ESO OWL, the 'OverWhelmingly Large' telescope). All of the proposed AO systems will have at least 5000 actuators to steer their deformable mirrors. This leads to very challenging requirements for future WFS that have been summarized in a white paper entitled "A Roadmap for the Development of Astronomical Adaptive Optics" [2]. The main points are the following:

1) Quantum efficiency $>80\%$ to detect dimmer guide stars
2) Detector array on the order of $512\times512$ pixels
3) Frame rate of 1 kHz or faster
4) Readout noise $<3$ electrons rms
5) Possibility to gate the detector for operation with artificial guide stars

Up to now, most WFS use fast frame-transfer CCDs, but points 2)-4) are not simultaneously achievable with the current CCD generation. Larger CCDs require faster clocking rates to achieve the high frame rates, but higher clocking speeds increase the readout noise. We propose a new detector / readout combination that can meet requirements 2)-5) with a quantum efficiency (QE) in excess of 35%. The lower QE seems to be acceptable as most if not all new telescopes will use bright laser guide stars.

## II. A PHOTON COUNTING MCP DETECTOR AS WFS

The basic detector concept we propose for our new WFS consists of the following main elements:

- a photocathode with high QE in the visible
- two MCPs in "chevron" configuration
- $2 \times 2$ Medipix2 event counting ASICs

In the photocathode the impinging photon releases a photoelectron. Up to now photocathodes in the optical showed only very modest QE, but progress in material development opens new application fields. Developments in commercial night vision tubes have demonstrated photocathode QE of $>40\%$ in the optical with GaAs photocathodes [3].

Thereupon the released photoelectron is proximity focused onto a matched pair of MCPs, where the signal is amplified. MCPs consist of an array of pores in a specialized glass substrate. The pore walls have a high secondary electron emission coefficient. Applying a high voltage across the MCP(s), the electron is accelerated, hits the pore wall releasing secondary electrons and finally causes an electron avalanche that exits the rear surface of the MCP. Microchannel plates combine many features of a good particle detector: high spatial resolution (pore diameters range from 2 $\mu$m upwards [4]), high gain (tunable from a few thousands to a few millions depending on the length-to-diameter ratio $L/d$ of the pores and the number of MCPs used in series), low dark current [5] and excellent timing resolution down to below 1 ns [6]. Two MCPs in a "chevron" configuration, where the pore angle gets reversed for the second plate with respect to the first, avoid ion feedback to the photocathode generated in the residual gas at the MCP output surface. We are planning to work with the MCP pair in a low gain configuration (gain of only 2-5$\times$10k) to assure the high rate capability of the detector. In addition MCPs are commercially available in various $L/d$ ratios and array sizes and at reasonable cost.

The key element of the proposed detector is the unique anode; MCPs are usually read out with centroiding anodes (crossed strip or delay lines [5]) that can detect the time and location of individual photon events ("photon counting"). However, for a future Shack-Hartmann WFS, the total detector

event rate would be 5000 (spots) x 1000 (photons/spot) x 1 kHz sampling rate = 5 GHz! Current photon counting readouts are limited to rates not much more than 5 MHz, a factor of 1000 less. The high required rate calls for a pixellated anode. Moreover, noiseless operation is desired. These considerations lead to the proposal to investigate the use of a bare CMOS event counting pixel chip as readout anode for the MCPs. The Medipix2 chip designed at CERN in the framework of the Medipix2 Collaboration [7] was chosen for this purpose.

### A. The Medipix2 photon counting ASIC

The Medipix2 chip consists of a matrix of $256 \times 256$ square pixels of 55 $\mu$m pitch. Each pixel comprises a charge-sensitive preamplifier, an upper and lower discriminator that can be used to select a signal window, and a 13-bit counter (Fig.3) [8]. Each pixel can be masked, tested electrically with a calibration pulse, and both thresholds can be tuned with 3 bits. Contrary to the operation with a connected semiconductor detector, where the threshold corresponds to a threshold in deposited energy, the threshold in the hybrid MCP - Medipix sets a cut related to the number of electrons collected at the pixel.
To be able to implement the mentioned functionality inside the tiny pixel area, 0.25 $\mu$m CMOS design technology was chosen. The measured equivalent input noise of Medipix2 is 100 $e^-$ rms, the residual threshold variation after tuning is also 100 $e^-$ rms. Typical threshold values are $\approx$2000 $e^-$ [8]. Because of the high ratio of threshold to noise there are no noise hits in the absence of an input signal.

For an acquisition, a programmable shutter signal is applied; as soon as the signal goes high again, readout starts. This shutter signal can be used to gate laser guide stars.

The chip can either be read out serially or using a parallel CMOS bus. In the latter case the complete matrix can be shifted out within 266 $\mu$s (at 100 MHz). As the electronics shutter is closed during readout, this means that at 1 kHz frame rate the detector will be active 73.4% of the time. Unlike CCD sensors, the readout process is completely noise-free as it is only a matter of shifting the counter bits out of the chip (fully digital readout).

Finally, Medipix2 is 3-side buttable. We are planning to use a 2×2 chip area for our final WFS ($\sim$260000 pixels).

To summarize, with the combination GaAs photocathode - MCP - Medipix2, we should be able to build a WFS that will fulfill the requirements of section I-A with a QE in excess of 35%.

## III. Measurement results

All the measurements in this paper were done with a small table-top experimental setup. The Medipix2 chip was wire-bonded to a chipboard. A matched pair of MCPs of 10 $\mu$m pore diameter on 12 $\mu$m spacing in chevron

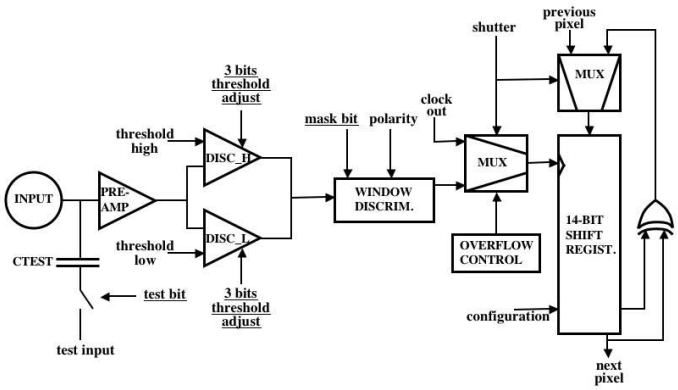


Fig. 3. Schematic diagram of a Medipix2 pixel cell. The charge collected at the input is amplified and shaped by the preamplifier block. An event gets counted if it exceeds the low threshold (and optionally if it is below the high threshold). The counter acts as well as a fast shift register to read out the pixel counts when the shutter signal goes high.

configuration was mounted approximately 500 $\mu$m in front of the Medipix2 chip. The detector was placed into a vacuum chamber that was pumped down to a few times $10^{-7}$ Torr. Our prototype MCP - Medipix2 detector did not have an optical photocathode. Instead of an illumination with photons in the visible wavelength region, the first experimental measurements were performed with UV photons to simplify the setup (MCPs have a small residual sensitivity to UV light in the $10^{-6}$ range). As described earlier, the optical sensitivity of the combination GaAs photocathode - MCP has already been proven, and in this paper we concentrate on the characteristics of the MCP - Medipix2 operation, leaving the detection efficiency measurements in the optical for later tests. For the UV measurements a pen-ray lamp with collimators (placed outside the chamber) illuminated the detector through a quartz window. With a bright UV source no photocathode is required. The electron images were acquired with beta sources placed inside the vacuum chamber.

Once all the main parameters have been fully explored, tube fabrication with the suitable photocathodes will be started.

### A. Measurements with UV photons

The detector described above was proposed by the authors in mid-2003, when it was not clear whether the method would work. The Medipix2 chip is a CMOS pixel readout chip designed to be bump-bonded to a semiconductor detector (Si, GaAs, CZT etc.) [9]. First, one had to prove that the charge cloud exiting the MCP could be detected by the frontend of the ASIC. Second, the hexagonal bump-bonding pad on each pixel is much smaller than the pixel itself (20 $\mu$m side-to-side). It was therefore necessary to show that uniform charge collection is feasible.

At about the same time two groups independently made the proposal to use a bare CMOS chip to detect the charge cloud

produced by a GEM or by Micromegas [10], [11]. In their case the charge cloud is produced from gas ionization and further multiplication.

The first measurements taken at short acquisition times showed isolated photon events of one count per hit pixel on the detector matrix. These events correspond to single photon events. The spot size is a function of [12]

- MCP gain
- rear field (between MCP exit and chip entrance surface)
- Medipix2 low threshold setting

This provides a few parameters to be tuned for the final WFS in order to get the best centroid precision.

To check the imaging uniformity, flood images were taken with the UV lamp. Individual events are integrated during the shutter-open time intervals and cannot be distinguished anymore. The voltage across the MCPs as well as the rear field were set to 1600 V/500 $\mu$m (60k gain of the MCP pair). For the image shown in Fig. 4 (left), the discriminator threshold was set just below 4000 $e^-$ and was increased by a factor of 10 for the image at the right. Two columns with shift register defects in the chip are visible as well as known dead spots (in white corresponding to zero counts) of the MCPs. The average number of counts per pixel is about 300 for both images.

It can be seen that the low threshold image is much more uniform. In the high threshold image multifiber bundles appear as well as a Moire pattern that is due to the imperfect alignment of the two MCP plates with respect to each-other. It can be explained by the fact that only high gain events are selected when using a high threshold. For such events the electrons coming from one hole in the top plate excite 2 or 3 holes of the bottom plate and the resulting (overlapping) charge cloud at the exit exhibits much higher gain and can be detected. This effect gets washed out at low thresholds or e.g. larger spot sizes. One can also apply appropriate corrections like multiplication with a flat field map. To reach approximately the same statistics in both images, the acquisition time for the right image had to be increased by more than a factor 80. It should be added that the right image does not correspond to normal operating conditions, but is of interest for the investigation of all effects in the full parameter space.

One of the main parameters that characterizes the performance of an imaging detector is its spatial resolution. For this purpose resolution masks are commercially available. Usually they consist of a certain number of line pairs per mm (lp/mm) both in x and y, where the line width is equal to the line spacing. We used the standardized 'Air Force' test pattern to determine the resolution of our detector. As can be seen in Fig. 5 (left), pattern 3-2 is just distinguishable. This corresponds to a resolution of 9 lp/mm, the theoretical limit (Nyquist limit) of a device with 55 $\mu$m pixels.

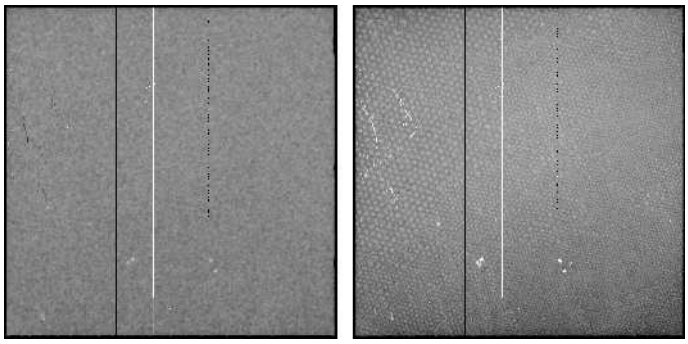

Fig. 4. Flood images taken with a UV pen-ray lamp. The right image had a 10 times higher discriminator threshold that brings out clearly Moire effects.

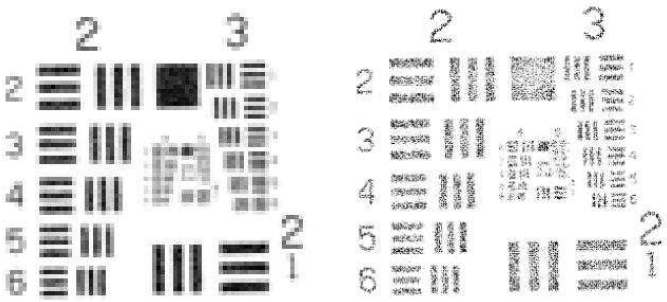


Fig. 5. Detail of the image of an Air Force test pattern illuminated with UV photons. The left image is uncorrected and yields the theoretical resolution limit of 9 lp/mm given by the 55 $\mu$m pixel size. On the right 1000 short acquisitions with max. 100-150 single photon events per chip were taken and the spot centroids plotted. This allows sub-pixel resolution to be achieved.

For low-rate imaging applications, one can make use of spot centroiding to achieve sub-pixel spatial resolution. To obtain Fig. 5 (right), we tuned the parameters in order to have larger event sizes of $\sim$12 pixels/event. 1000 frames of short acquisition time (to avoid overlapping events) were taken. A program then identified each spot and calculated its center. The right figure is a 2D representation of the centroid positions of the 1000 frames. It results in a clear improvement of the resolution to almost 18 lp/mm (group 4-2 starts to be resolved), which would be the theoretical resolution of a detector with 28 $\mu$m pixels.

*1) Simulating a Shack-Hartmann WFS:* As described before a Shack-Hartmann WFS relies on the exact localization of individual spots. Movements of the spots indicate changes in the atmospheric conditions. To simulate such a situation, we used an image mask (an electroformed Ni sheet with a 10 $\mu$m diameter pinhole array at 500 $\mu$m spacing in both directions) between the light source, a UV pen-ray lamp with 2 mm aperture, and the detector. The pinhole mask was fixed about 2.5 mm above the input MCP, and the lamp was at about 50 cm distance. There were approximately 700 pseudo-stellar images produced on the detector in a grid that was slightly rotated relative to the Medipix2 readout pixels (see Fig. 6). The white areas in the image are due to some small pieces of kapton tape

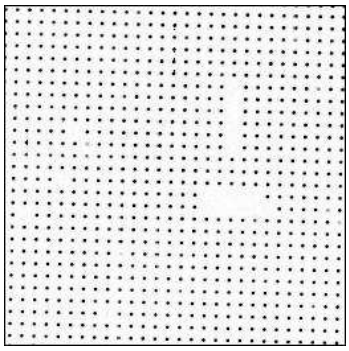

Fig. 6. Image obtained with a uniformly spaced pinhole array of 10 $\mu$m diameter pores. The UV lamp simulated the guide star and the image mask simulated the lenslet array used with Shack-Hartmann WFS.

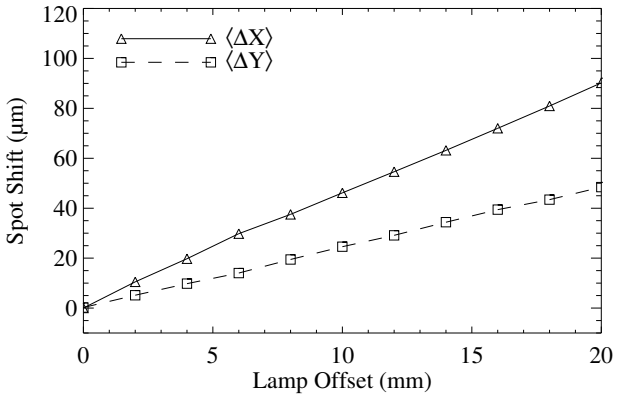


Fig. 7. x- and y-shifts for the 700 spots at each lamp location show a good linear response. The width of the 700-spot distributions amounted on average to only 3 $\mu$m.

left over on the image mask.

Data was acquired with a MCP gain of about 60 ke$^-$ per detected photon and 1600 V/500 $\mu$m rear field to restrict the lateral spread of the charge cloud exiting the MCPs small. The 25 s integration time resulted in about 600 photons per spot. Each data run consisted of two integrations taken at each of 11 lamp locations on 2 mm increments from 0 to 20 mm and aimed at investigating the spot movement. The x and y locations of each spot were found by fitting a Gaussian to the x and y profiles of a $9 \times 9$ pixel area surrounding each spot. For each lamp offset the location of each spot was compared to its location in the first image (the 0 mm lamp position) and the x- and y-shifts calculated. The result is plotted in Fig. 7 and shows the good sub-pixel spatial linearity of the detector in both directions. The measurement points for each lamp location correspond to the fitted value of the shift for all 700 spots at this position; the sigma of these distributions ranged between 2 and 4 $\mu$m only. This sigma variation had a frequency of exactly 55 $\mu$m (the pixel pitch) and is due to undersampling. It disappears with lower rear field and therefore larger spot sizes.

### *B. First measurements with electrons*

For AO applications it is necessary to fabricate tubes with photocathodes to convert the incoming optical photons into electrons. For certain applications in various other fields electrons have to be detected. Without an optical photocathode the detector would be relatively simple, and an open-faced detector, operating in a vacuum of less than $10^{-6}$ Torr, could be designed and fabricated now. Therefore we tried to evaluate its performance for direct electron detection with two beta sources of different maximum energies.

Fig. 8 shows two flood fields taken with beta sources. For the left image a $10 \times 30$ mm strip $^{63}$Ni source with 67 keV endpoint energy was used and for the right image we used a $^{204}$Tl source of 10 mm diameter with 764 keV endpoint energy. The same detector settings were applied as for Fig. 4 (right). The left image contains in average 300 counts/pixel and the Tl image 100 counts/pixel. Again some Moire effects are visible as well as the dead spots of the MCPs. It should be pointed out that the images are very similar, and show that high rate imaging of high energy electrons at spatial resolutions of $\sim$9 lp/mm is achievable with this detector.

Moreover, an attempt was made to evaluate the QE of the two beta images. For this purpose a low threshold around 4000 e$^-$ was used and 10 images taken with an acquisition time chosen such that single events could be distinguished (about 150 spots/image). Counting these spots and comparing the resulting number to the expected event rate (derived from the activity of the source, its distance to the detector and a rough estimation of the solid angle) yielded a QE of 46% (Ni image) and 63% (Tl image). These numbers should be treated as rough estimation only; the error in this value could be as large as 20% mainly due to our geometry assumptions (the sources were assumed to be point sources which is not the case). Nevertheless the order of magnitude and the increase of QE with energy (detection efficiency increases with energy for beta energies above approximately 50 keV, when the electrons are energetic enough to traverse the MCP wall and reach another MCP channel) is consistent with literature [13]. It should be noted here that the MCP efficiency to beta particles is lower than its sensitivity to photoelectrons emitted from a photocathode like in the adaptive optics application, as in that case one can accelerate the photoelectrons to optimal energy (around 200-500 eV), where the detection efficiency of the MCP will almost reach 100% (disregarding the geometric open area ratio).

These first results open the way to study new possible application fields like a beam monitor for hadron therapy that detects secondary electrons emitted from a thin foil placed in the beam (the principle is explained in [14]). Other possible applications could include a Cherenkov light detector, a UV detector for synchrotron applications or a detector related to 'synchrotron microscopes'. There the object to be studied is bombarded with focussed X-rays, and the detector has to

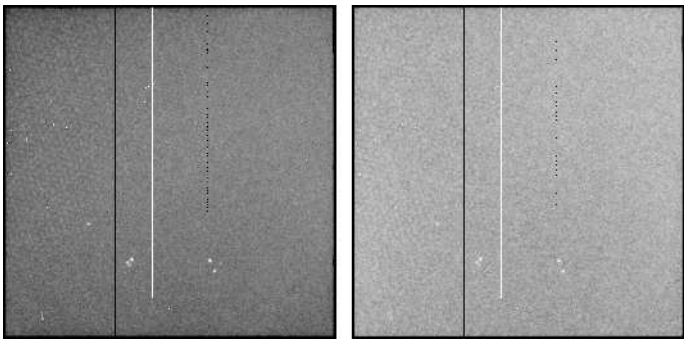

Fig. 8. Flood images taken with a $^{63}$Ni (left) and a $^{204}$Tl (right) beta source. These images are very similar to the UV flood image of Fig. 4.

measure the angular distribution of the electrons emitted from the object that have passed through an analyzer.

## IV. Conclusion

This paper presents a novel detector concept based on a photocathode, microchannel plates and the Medipix2 counting CMOS pixel chip as readout anode. Various detector aspects were discussed mainly in view of the target application, a Shack-Hartmann wavefront sensor for adaptive optics. The spatial resolution of the detector was shown to be equal to the Nyquist limit for UV photons. Subpixel resolution can be obtained for low rate applications using spot centroiding. Flood fields with beta sources indicate that this detector has a great potential to be used over a wide range of wavelengths with several types of radiation. Detectable radiation ranges from optical photons over UV, X-rays, electrons, ions and neutrons.

## Acknowledgment

The authors wish to thank the Medipix Collaboration for the Medipix2 chips, readout hardware and software and for valuable advice. Some of the authors (J.V., J.McP., A.T. and O.S.) would like to acknowledge support of AURA through the NSF under AURA cooperative agreement #AST-0132798-SPO#6 (AST-0336888).

## References

[1] R. K Tyson, "Introduction to Adaptive Optics", *SPIE Press*, Bellingham, Washington, USA, 2000.

[2] R. Angel *et al.*, "A Roadmap for the Development of Astronomical Adaptive Optics", July 6, 2000, Available: http://www.noao.edu/dir/ao/ .

[3] Online: http://www.ittnv.com/itt/Active/SpecLeftMenu/SpecialtyProds .

[4] J. Vallerga, J. McPhate, B. Mikulec, A. Tremsin, A. Clark and O. Siegmund, "Noiseless imaging detector for adaptive optics with kHz frame rates", presented at the SPIE conference Astronomical Telescopes and Instrumentation 2004, June 21-25 2004, Glasgow, UK, *submitted for publication in SPIE Proceedings*.

[5] O. H. W. Siegmund, A. S. Tremsin, J. V. Vallerga, "Advanced MCP sensors fur UV/visible astronomy and biology", *Nucl. Intr. and Meth. A*, 510 (2003) 185-189.

[6] J. Vallerga and J. McPhate, "Optimization of the readout electronics for microchannel plate delay line anodes", *Proc. SPIE*, 4139 (2000) 34-42.

[7] Online: http://medipix.web.cern.ch/MEDIPIX/ .

[8] X. Llopart, M. Campbell, R. Dinapoli, D. San Segundo and E. Pernigotti, "Medipix2, a 64k pixel readout chip with 55 $\mu$m square elements working in single photon counting mode", *IEEE Trans. Nucl. Sci.*, vol. 49, 2279-2283, October 2002

[9] B. Mikulec, "Development of segmented semiconductor arrays for quantum imaging", *Nucl. Intr. and Meth. A*, 510 (2003) 1-23.

[10] H. van der Graaf *et al.*, "The readout of a GEM or Micromegas-equipped TPC by means of the Medipix2 CMOS sensor as direct anode", *Nucl. Intr. and Meth. A*, 535 (2004) 506-510.

[11] R. Bellazzini *et al.*, "Reading a GEM with a VLSI pixel ASIC used as a direct charge collecting anode", *Nucl. Intr. and Meth. A*, 535 (2004).

[12] J. Vallerga, J. McPhate, B. Mikulec, A. Tremsin, A. Clark and O. Siegmund, "Optically sensitive Medipix2 detector for adaptive wavefront sensing", presented at the IWORID conference 2004, July 25-29 2004, Glasgow, UK, *submitted for publication in Nucl. Instr. and Meth. A*.

[13] M. I. Babenkov, V. S. Zhdanov and S. A. Starodubov, "Chevron of microchannel plates as position-sensitive detector for $\beta$-spectrometers", *Nucl. Instr. and Meth. A*, 252 (1986) 83-86.

[14] L. Badano *et al.*, "SLIM, an innovative non-destructive beam monitor for the extraction lines of a hadrontherapy centre", these proceedings.